NASA/TP-2000-210639

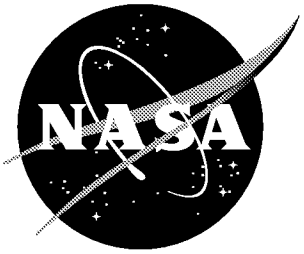

Characteristics of Extrinsic Fabry-Perot Interferometric (EFPI) Fiber-Optic Strain Gages

David A. Hare and Thomas C. Moore, Sr.
Langley Research Center, Hampton, Virginia

December 2000

The NASA STI Program Office ... in Profile

Since its founding, NASA has been dedicated to the advancement of aeronautics and space science. The NASA Scientific and Technical Information (STI) Program Office plays a key part in helping NASA maintain this important role.

The NASA STI Program Office is operated by Langley Research Center, the lead center for NASA's scientific and technical information. The NASA STI Program Office provides access to the NASA STI Database, the largest collection of aeronautical and space science STI in the world. The Program Office is also NASA's institutional mechanism for disseminating the results of its research and development activities. These results are published by NASA in the NASA STI Report Series, which includes the following report types:

- TECHNICAL PUBLICATION. Reports of completed research or a major significant phase of research that present the results of NASA programs and include extensive data or theoretical analysis. Includes compilations of significant scientific and technical data and information deemed to be of continuing reference value. NASA counterpart of peer-reviewed formal professional papers, but having less stringent limitations on manuscript length and extent of graphic presentations.

- TECHNICAL MEMORANDUM. Scientific and technical findings that are preliminary or of specialized interest, e.g., quick release reports, working papers, and bibliographies that contain minimal annotation. Does not contain extensive analysis.

- CONTRACTOR REPORT. Scientific and technical findings by NASA-sponsored contractors and grantees.

- CONFERENCE PUBLICATION. Collected papers from scientific and technical conferences, symposia, seminars, or other meetings sponsored or co-sponsored by NASA.

- SPECIAL PUBLICATION. Scientific, technical, or historical information from NASA programs, projects, and missions, often concerned with subjects having substantial public interest.

- TECHNICAL TRANSLATION. English-language translations of foreign scientific and technical material pertinent to NASA's mission.

Specialized services that complement the STI Program Office's diverse offerings include creating custom thesauri, building customized databases, organizing and publishing research results ... even providing videos.

For more information about the NASA STI Program Office, see the following:

- Access the NASA STI Program Home Page at http://www.sti.nasa.gov

- E-mail your question via the Internet to help@sti.nasa.gov

- Fax your question to the NASA STI Help Desk at (301) 621-0134

- Phone the NASA STI Help Desk at (301) 621-0390

- Write to:
  NASA STI Help Desk
  NASA Center for AeroSpace Information
  7121 Standard Drive
  Hanover, MD 21076-1320

NASA/TP-2000-210639

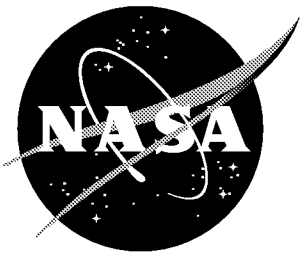

Characteristics of Extrinsic Fabry-Perot Interferometric (EFPI) Fiber-Optic Strain Gages

David A. Hare and Thomas C. Moore, Sr.
Langley Research Center, Hampton, Virginia

National Aeronautics and
Space Administration

Langley Research Center
Hampton, Virginia 23681-2199

December 2000

Available from:

NASA Center for AeroSpace Information (CASI)
7121 Standard Drive
Hanover, MD 21076-1320
(301) 621-0390

National Technical Information Service (NTIS)
5285 Port Royal Road
Springfield, VA 22161-2171
(703) 605-6000

Abstract

The focus of this paper is a comparison of the strain-measuring characteristics of one type of commercially available fiber-optic strain sensor with the performance of conventional resistance strain gages. Fabry-Perot type fiber-optic strain sensors were selected for this testing program. Comparative testing is emphasized and includes load testing at room temperature with apparent strain characterization cryogenically and at elevated temperatures. The absolute accuracy of either of these types of strain gages is not addressed.

Introduction

Langley Research Center (LaRC) uses strain gages in many varied and challenging test environments. As testing scenarios become more demanding, not only at Langley but at other testing centers, there is the realization that current strain gage technology does not and cannot provide a reasonable means for measuring strain when certain testing requirements are encountered. A relatively new type of strain sensor, the "fiber-optic" (F-O) strain gage, offers the promise of making strain measurements where resistance-type strain gages fail to provide the desired features. Manufacturers of F-O strain gages state the following advantages when using their strain sensor: immunity to electromagnetic interference, immunity to leakage-to-ground problems, and no inaccuracies associated with long, multiple, signal lead requirements. The fiber-optic strain gage's lower mass provides a significant weight savings. Also, this reduced mass in the F-O gage minimizes reinforcing effects that conventional strain gages can induce in a test article. Most of these stated advantages with the F-O gages are the typical shortcomings of the resistance gages, especially where flight testing or "testing in the field" is involved.

There are several types of fiber-optic strain gages, two of which comprise the majority of commercially available strain sensors. The most popular manufacturing method produces the Fabry-Perot strain sensor with the second most popular type being the Bragg-grating strain sensor. This paper presents a comparison of performance characteristics between the Fabry-Perot type fiber-optic strain gage with a widely used conventional resistance strain gage. As described by Tran, the Fabry-Perot type of sensor uses a phase difference or "shift" between reference and sensing reflections of the fibers for making strain measurements [1]. This phase shift described by Tran and others is then used to calculate strain. In the world of structural and/or materials testing, the means to generate real-time data in engineering terms is a practical necessity. This "necessity" is addressed by Tran, et al, in another paper in which a means of measuring absolute strain in real time is described [2]. In this paper, comparative data with a conventional resistance strain measurement system and a dedicated "strain measuring system" for a Fabry-Perot type strain sensor (with its fiber-optic gages inclusive) will be presented. The ability of the F-O strain measuring system and its gages to measure strains comparative to resistance gages will be discussed.

A brief description of this type of F-O gage is provided in the paper. Comparative testing includes load testing at room temperature with apparent strain characterizations cryogenically and at elevated temperatures. Although some load tests are performed with the fiber-optic gages in compression, the primary configuration is in tension. Test results are presented as phase 1 testing and phase 2 testing. Presenting test results in two phases is due to the manufacturer's change in the manufacturing process as the first group of gages was being tested. Note that the manufacturer of the gages offered an improved F-O sensor as the first group of gages was being evaluated. It was decided to procure these "improved" gages and test them as part of this effort. Thus, data from phase 1 testing are generated from the first

group of gages procured for this effort, and data from phase 2 testing are generated from the second group of gages procured.

Fabry-Perot Fiber-Optic Strain Gage

The fiber-optic gages presented here are commercially-available and employ an Extrinsic Fabry-Perot Interferometric (EFPI) technique to measure the displacement between two optical fibers. A typical gage consists of a primary and a secondary polyimide-coated fiber (fig. 1). The fibers are inserted into each end of a capillary tube. A cavity of approximately 55 μm remains between the primary and secondary fibers. Each optical fiber is then attached at each end of the capillary tube by using an adhesive. The distance between these two attachment points and the gap between the optical fibers determines the gage factor for the sensor. The primary fiber serves as the transmit/receive fiber for a light source containing multiple frequencies. The end of the primary fiber is approximately 4 percent reflective, allowing some light to be reflected toward the receiver. The remaining light that passes through the 4 percent reflector is then reflected to the receiver by the secondary fiber that, for the purposes of this paper, is approximately 100 percent reflective. This system provides two reflected waves of light. As the fiber is strained, the displacement between the two fibers changes from its initial position. A change in the displacement induces phase differences between the reflected waves. These phase differences produce a variety of fringe patterns as a function of displacement. By using interferometric techniques, these fringe patterns determine the amount of change in the linear displacement seen by the gage. This change in displacement is strain. In a traditional EFPI demodulation scheme where the sensor is illuminated by a monochromatic source, the linear displacement of the air-gap can be determined by monitoring the phase of the output intensity, I, defined as:

$$\frac{I_r}{I_i} = \frac{2R(1-\cos\phi_0)}{1+R^2-2R\cos\phi_0} \tag{1}$$

where

$$\phi_0 = \frac{4\pi n_0 d}{\lambda_s} \tag{2}$$

is the round trip optical path length difference, R is the reflectivity of the fiber endfaces, d is the air-gap width separation, n_0 is the refractive index of air, and λ_s is the wavelength of the laser. If the EFPI sensor is used with a broadband source, as with the data system used for the testing, the gap separation of the Fabry-Perot can be calculated from the equation:

$$d = \frac{\Delta\phi\lambda_1\lambda_2}{4\pi\Delta\lambda} \tag{3}$$

where $\Delta\lambda$ is the difference of two wavelengths detected by the spectrum analyzer, and $\Delta\phi$ is the associated phase difference between them [2][3]. Examination of Eq. (3) reveals that the change in wavelength of the return signal as a function of the strain is linear.

Evaluation of EFPI Embedment Fiber-Optic Strain Gage (Phase 1 Testing)

Instrumenting Test Beams for Testing

The three fiber-optic strain gages that were tested during phase 1 were installed on two 17-4 steel cantilever-type test beams, designated 69C and 78C. Initially, each test beam was instrumented with one widely-used conventional resistance strain gage and one Fabry-Perot fiber-optic strain gage. A photograph showing an installed fiber-optic gage on a test beam is shown in figure 2. Installation techniques used on the resistance strain gages were also used on the fiber-optic strain gages [4] [5]. The installed gages were then cured in a temperature chamber for two hours at 150°F. Following the cure cycle, a final inspection of the installation was conducted and the gage locations were recorded. As previously stated, this process was duplicated for the strain gage installations on both test beams. After initial load data were collected from the fiber-optic and resistance strain gages installed on test beam 69C, the third fiber-optic strain gage was installed adjacent to the previously installed fiber-optic gage on this beam. This third gage provided data on the repeatability of the measured strain by using two gages on one beam.

Test Apparatus and Data Acquisition

Load tests were performed on the strain-gaged test beams by using a standard laboratory-type cantilever loading fixture and deadweights. For each test beam that was tested, the resistance strain gage was connected to a bridge completion unit forming a Wheatstone Bridge circuit with one active arm. The fiber-optic strain gage was connected to a fiber-optic strain indicator and signal-conditioning unit purchased from the manufacturer that furnished the fiber-optic gages. Output signals from the fiber-optic data system and the Wheatstone Bridge circuit were read by using an HP 3457A multimeter and were recorded on a laboratory computer through an IEEE 488 interface.

Test Procedure

The preliminary test procedure for the evaluation of the EFPI fiber-optic strain gage consisted of conducting room temperature static loads on each of the instrumented test beams. Each test article was sequentially loaded/unloaded up to 10 lb in 1-lb increments, resulting in a maximum strain of approximately 950 micro-strain. This load schedule was replicated three times for each strain gage on each test beam. Comparisons were then made between the recorded strain readings taken with the resistance strain gages to those recorded strain readings taken with the fiber-optic strain gages. Note that the plots in figures 3, 4, and 5 show a "calculated strain" along with the other data.

$$\sigma = \frac{Mc}{I} \tag{4}$$

It can be shown from Equation 4 that the bending stress σ for a cantilevered beam is directly proportional to the distance c (distance between a "fiber" in the test beam and neutral axis of the test beam) and the bending moment M. The bending moment M for a rectangular cantilevered beam is the product of a known force W that is applied at a given distance L from a reference point. The reference point in this case is the geometric center of the strain gage along the centerline of the principal axis of the strain gage. In addition, the moment of inertia I of the rectangular-shaped test beam about its own centroidal axis is needed and is calculated using the equation

$$I = \frac{bh^3}{12} \tag{5}$$

$$c = \frac{h}{2} \tag{6}$$

where b is the width of the test beam at the location of the strain gage and h is the test beam thickness at the location of the strain gage. Since the amount of stress located at the surface of the test beam is required, in Equation 4 the variable c represents the distance between the outer most "fiber" and the neutral axis [6]. By knowing the modulus of elasticity of the test beam and by substituting equations 5 and 6 into equation 4 to obtain the stress, the strain can be calculated as a function of the applied load using equation 7.

$$\in = \frac{6WL}{Ebh^2} \tag{7}$$

This calculated strain was based on the thickness of the test beam without consideration for any error that would be generated due to the finite thickness of the gages, which positioned them slightly above the beam surface.

Load Testing Results and Discussion

The room temperature load data recorded with test beam 69C indicated that the fiber-optic strain gage (Serial No. K990261) measured approximately 27 percent higher strain, for a given load, than the resistance strain gage. These data are shown in figure 3. In table 1.1, the calculated strain values are listed along with the measured strain values from the fiber-optic and resistance strain gages that were tested. The calculated strain that the resistance strain gage should have measured was calculated based on the physical location of the strain gage, the size and modulus of the test beam, and the deadweight load applied at a given distance from the gage. The calculations ignored the fact that the sensors were slightly above the beam surface because of the actual gage thickness. The center of the fiber-optic strain sensor was located approximately 0.007 inches above the surface of the test beam. The test beams that were used for these laboratory tests had a thickness h of 0.131 inches. The strain measured by the fiber-optic sensor is based on the value c, which is represented by half the thickness of the test article plus the distance (or height) from the test beams surface to the center of the strain sensing area of the fiber-optic sensor. With the strain sensing area of the sensor positioned 5.3 % higher above the surface of the test article than the test articles thickness, according to Eq. (4), the stress that the sensor is subjected to will be 5.3 % higher. Since stress and strain are linear functions of one another, and are directly proportional to one another, the strain at the sensing area of the sensor must also increase by the same percentage as the stress. It is evident from the data shown in table 1.1 that the strain measured by the resistance gage is much closer to the calculated strain than the strain measured by the fiber-optic strain gage. A second fiber-optic strain gage (Serial No. K990263) was installed adjacent to the first gage and load data were obtained. Data measured with this second fiber-optic gage indicated a 30 percent higher measured strain than the strain measured with the resistance strain gage. A comparison of the load data listed in table 1.1 for the two fiber-optic gages indicated that the strain measurements from each gage differed by 24 micro-strain or 2.1 percent. This difference is reflected in figure 3. Note that the respective gage factors, furnished by the manufacturer for these two fiber-optic gages, differed by 2.4 percent. The room temperature load data acquired from test beam 78C produced results similar to those obtained from load tests conducted on test beam 69C. These data indicated that the strain levels measured with the fiber-optic gage (Serial No. K990262) were 25 percent higher than the strain levels measured by the resistance strain gages. Based on these differences, the stated gage factor of the fiber-optic gage was set 25 percent higher, and additional load data were obtained by using this "corrected" gage factor. The results are

shown in figure 4. The data with the adjusted gage factor confirmed that the fiber-optic gages will read strains comparable to conventional gages when the gage factor is properly set. The fiber-optic strain measurements recorded from each gage that was tested were consistently higher, for a given load, than those measurements made by using the resistance gage. Strain measurements taken with the resistance strain gages for both test beams fell within 3.2 percent of the calculated strain for each beam. The measured strain from the fiber-optic gages was significantly higher than the calculated strain levels. The data reflecting the repeatability of the fiber-optic gages that were tested on cantilever test beams (69C and 78C) are shown in figures 6 and 7. Data that are represented in these figures were calculated by averaging three sets of load data, from both the fiber-optic and resistance strain gages, and then by subtracting their respective averages from each data set. Of the three fiber-optic gages tested during phase 1 of this project, the largest standard deviation, based on three load replications, was ±0.635 micro-strain. The smallest standard deviation was ±0.294 micro-strain. If this standard deviation were related to the "as tested" full-scale outputs of 1120 micro-strain and 1174 micro-strain, respectively, the repeatability varied between ±0.057 percent and ±0.025 percent.

The laboratory test results obtained from phase 1, shown in table 1.1, indicated that the measured strain between the resistance and fiber-optic strain gages differed by 25 to 30 percent. The resistance and fiber-optic gages were tested on the same test articles by using the same installation techniques and adhesives. Based on the three fiber-optic gages that were tested, the repeatability of the gages varied between ±0.025 and ±0.057 percent, corresponding to <±0.3 and <±0.7 micro-strain, respectively. All stated percentages related to the repeatability of the strain gages were calculated based on one standard deviation. The gage factor was inversely proportional to the amount of measured strain. The relationship between the strain measurement taken from the fiber-optic gage and its stated gage factor were linear functions of one another. Therefore, based on the data shown in figure 4, if the gage factor were changed by a given percentage, the strain measured by that gage would inversely change by the same percentage. The load data that were obtained from both test beams (69C and 78C) support the argument that the particular manufacturer of these fiber-optic gages could not accurately state the gage factor for their gages. The manufacturer was notified of the findings pertaining to the potential error in their stated gage factor. The manufacturer then responded by indicating that they were considering incorporating an improvement into their manufacturing processes that would enable them to furnish the user with a more accurate stated gage factor. This improvement would provide a more accurate measurement of the distance between the two attachment points for the fibers at either end of the capillary tube. It is this distance that defines the gage factor, that is, the sensitivity of the sensor.

Table 1.1. Phase 1 Cantilever Test Beam Load Data

Test beam designations	Calculated ($\mu\epsilon$)	Fiber-optic gages			Resistance gage
		Serial no. K990261 ($\mu\epsilon$)	Serial no. K990262 ($\mu\epsilon$)	Serial no. K990263 ($\mu\epsilon$)	CEA-06-125UW-350 ($\mu\epsilon$)
69C	900	1109	-	1133	871
78C	952	-	1174	-	940

Evaluation of "Improved" EFPI Embedment Fiber-Optic Strain Gage (Phase 2 Testing)

Scope of Phase 2 Testing

The primary focus for phase 2 of this test evaluation program was improvements that could be made to ensure a more accurate determination of the strain measured by using Fabry-Perot fiber-optic strain sensors. The areas of possible improvement to be addressed were the installation procedures used for the fiber-optic gages, and more importantly, the improvements the manufacturer had now incorporated to provide a better determination of the stated gage factor for the gages. In addition to load testing, phase 2 included apparent strain characterizations. Based on improvements made during the manufacturing process, new fiber-optic strain gages were procured from the same manufacturer. These additional gages had the manufacturer's stated gage factors that were obtained by using a new improved displacement measurement technique for determining the gage factor. To determine whether any improvements in the fiber-optic gage's accuracy could be realized from the manufacturing improvements that were made, laboratory tests were conducted with these improved gages on the same test articles that were used throughout phase 1 of this testing program. Several laboratory-standard constant strain test beams were also instrumented with these improved fiber-optic gages and conventional resistance gages. These beams were used for obtaining additional load data and determining apparent strain characteristics for the fiber-optic gages.

Instrumenting the Two 17-4 Cantilever Test Beams

The two cantilever test beams that were instrumented in phase 1 for load testing had the "new and improved" fiber-optic strain gages, again from the same manufacturer, added for phase 2 testing. The installation procedure and adhesive were modified for this portion of the testing program. The beams were chemically cleaned in the same manner as for the phase 1 testing. The fiber-optic gages were installed by gently placing the gage in position on the test beam surface. Kapton-based tape was then used to secure each end of the gage to the surface of the test beam. The Kapton-based tape was placed on the fiber, approximately 90 mils away from either end of the capillary tube. Once the fiber-optic strain gage was secured in place with the Kapton-based tape, the bonding agent, AE-15 from Measurements Group, was applied to the gage and the substrate by using a custom wooden applicator. The application of the adhesive provided a void-free glue line that extended approximately 50 mils beyond the ends of the capillary tube. Natural capillary action drew the bonding agent under the gage and along the fiber. The gage installation on test beam 69C was cured for four hours at 150°F. Due to time constraints, the gage installation on test beam 78C was cured for two hours at 225°F.

Test Procedure for Cantilever Beams

The test procedures and the data acquisition system that were used in the phase 1 testing were also used in the phase 2 testing of the EFPI fiber-optic strain gage. Load testing consisted of room temperature static loads on each of the instrumented test beams (69C and 78C). Each test article was sequentially loaded/unloaded up to 10 lb in 1-lb increments, resulting in a maximum strain of approximately 950 micro-strain at the gage. This load schedule was replicated three times for each strain gage. Comparisons were then made between the strain readings from the resistance strain gages to those readings taken from the improved fiber-optic strain gages that were installed. The data from the improved fiber-optic strain gages were compared to those strain measurements that were previously recorded with the original fiber-optic gages and the resistance gages.

Load Testing Results for Cantilever Beams

The room temperature load data recorded during phase 2 testing with test beam 69C indicated that data with the fiber-optic strain gage (K990505), shown in Figure 3, measured approximately 12.5 percent higher strain than the resistance strain gage which is still quite large. In table 2.1, the calculated strain values are listed with the measured strain values from the fiber-optic and resistance strain gages that were tested. It is evident from the data shown in table 2.1 that the strain measured by the resistance gage is much closer to the calculated strain than the strain measured with the fiber-optic strain gage. The room temperature load data that were acquired with test beam 78C produced significantly different results than those obtained from the load tests conducted on test beam 69C. The Fiber-Optic strain gage (K990506) data recorded from test beam 78C indicated a 1.2 percent higher measured strain compared to the strain measured with the resistance strain gage. Comparing the load data recorded in phase 1 with data obtained during phase 2 testing with both test beams (69C and 78C) suggests that the errors in the fiber-optic gage's stated gage factor were significantly reduced. The data reflecting the repeatability of the fiber-optic gages tested on cantilever test beams 69C and 78C are shown in figures 6 and 7. The largest recorded standard deviation, based on three load replications, was ±0.545 micro-strain. The smallest standard deviation was ±0.518 micro-strain. If this standard deviation were related to the full-scale outputs of 982 micro-strain and 950 micro-strain, respectively, the repeatability would be ±0.055 percent.

Table 2.1. Phase 2 Cantilever Test Beam Load Data

Test beam designations	Calculated (με)	Serial no. K990505 (με)	Serial no. K990506 (με)	CEA-06-125 UW-350 (με)
69C	900	982	-	873
78C	952	-	950	939

Instrumenting the Constant Strain Test Beams

Each of the 18.5 percent maraging steel (Vascomax 200) constant strain test beams that were instrumented and tested were numbered Beam 200-2 and Beam 200-3, respectively. The testing temperature range (−150°F to +325°F) dictated that the type of resistance strain gage used for testing would be changed from Measurements Group, Inc. type CEA-06-250UW-350 to Measurements Group, Inc. type WK-06-125AD-350. The bonding agent used for the resistance gage was also changed from EPY-150 to Measurements Group, Inc. type M Bond 610. The beams were chemically cleaned in the same manner as they had been for previous gage installations. The resistance gage was cured for one hour at 340°F with 60 psi of pressure applied to the gage. This installation procedure used for the resistance strain gages was followed for both constant strain test beams. Initially, each constant strain test beam was instrumented with one resistance gage and one fiber-optic gage, K990484 and K990483, respectively. A photograph showing a typical resistance gage and fiber-optic gage installation on these test beams is shown in figure 2. After load and apparent strain testing were completed on these gages, additional fiber-optic gages were installed on both constant strain test beams. One additional fiber-optic gage (K990482) was installed on test beam 200-2 adjacent to the first. To quantify the scatter in the strain measured from one fiber-optic gage to another, three additional fiber-optic gages were installed on test beam 200-3. In addition, the newly installed fiber-optic strain gages installed on test beam 200-3 were installed so that the gages could be statically load tested in compression. Each fiber-optic gage was installed by gently placing the gage in position on the test beam surface. The installation of fiber-optic

strain gage K990484 was secured at each end with Kapton-based tape, and the bonding agent, EPY-500 from BLH Electronics, Inc., was applied to the gage and the substrate by using a custom wooden applicator. The application of the adhesive provided a void-free glue line that extended approximately 50 mils beyond the ends of the capillary tube. A constant 10 to 15 psi of pressure was applied to the fiber-optic gage during the cure cycle. The fiber-optic gage installation on test beam 200-2 was cured for four hours at 250°F. Following the cure for the fiber-optic gage, both the resistance gage and the fiber-optic gage were post cured for two hours at 340°F. The technique used for installing the additional fiber-optic gage K990482 differed from the technique used for K990484. The bonding agent used for the additional gage installation was AE-15 from Measurements Group, Inc. Additionally, the gage installation was cured for two hours at 225°F without pressure applied to the installation during the cure cycle. The installation of fiber-optic gage K990482 was also post cured for two hours at 300°F. The reason for the change in the type of bonding agents that were used during the course of testing was due to the availability of a particular adhesive.

Procedure for the Constant Strain Beams Testing

The previous deadweight loading procedures were limited to stress levels ranging from 25000 to 27 000 psi. This stress limit was due to a concern that large test beam deflections at higher stress levels could result in the gages exhibiting a nonlinear response. The use of the Vascomax 200 constant strain test beams allowed for testing of the EFPI fiber-optic strain gages at much higher strain levels. Load testing consisted of room temperature static loads on each of the instrumented test beams (200-2 and 200-3). Each test beam was sequentially loaded/unloaded up to 25 lb in increments of 5 lb, resulting in a maximum strain of approximately 3000 micro-strain. This load schedule was replicated three times for each strain gage. Strain readings from the resistance strain gages and readings from the improved fiber-optic strain gages that had been installed were then compared.

Load Testing Results for the Constant Strain Beams

The strain measurements recorded by using the fiber-optic strain gage (K990484) that was installed on test beam 200-2 were approximately 3.9 percent higher than the strain measured with the resistance strain gage. The strain measured with the second fiber-optic gage (K990482) that was also installed on test beam 200-2 measured 7.4 percent higher strain than the strain measured with the resistance gage (data shown in table 2.2). The strain measured with the fiber-optic gage K990483 that was installed adjacent to the resistance gage on test beam 200-3 produced similar results. Load data obtained from these two test beams are referred to in figures 5 and 8. The strain measurements taken with the three fiber-optic gages installed adjacent to one another on test beam 200-3 exhibited an 85 micro-strain variation between them. These fiber-optic strain gages were tested to a nominal full-scale of 3150 micro-strain. Since the resistance strain gage was tested in tension, and three of the four fiber-optic gages that were tested on test beam 200-3 were tested in compression, the absolute value of the strain measurements are represented in figure 5. The differences between the strain measured with the fiber-optic and resistance gages are significantly smaller than initially measured with phase 1 testing. Although there is a significant decrease in the differences between the strain measured with the resistance gages versus the fiber-optic gages, there are noticeable inconsistencies in the strain measured from one fiber-optic gage to another. The indication is that even though the manufacturer of these gages has made improvements, the gage factors are still not precisely determined for their fiber-optic gages.

Apparent Strain Characterization of Fiber-Optic Strain Gage

An integral part of evaluating the performance of EFPI fiber-optic strain gages was characterizing the output signature of these gages as a function of temperature change. The thermally generated output from these fiber-optic strain gages, for this paper, shall be referred to as "apparent strain." Apparent strain characterization tests were conducted by using an uncompensated fiber-optic strain gage (K990484) that was installed on the Vascomax 200 constant strain test beam 200-2. The elevated temperature apparent strain data that were obtained with the fiber-optic gage were essentially linear (fig. 9). A linear regression on the elevated temperature data, represented in figure 9, reflected a slope of 4.11 micro-strain/°F. Although a second-order term was present in the data set, it was relatively small. The cryogenic temperature apparent strain data, shown in figure 10, were obtained with this same fiber-optic gage. The slope of the linear regression on the data was 3.6 micro-strain/°F. It is evident from figures 9 and 10 that the apparent strain for the fiber-optic strain gage was linear over a wide temperature range. The repeatability of three sets of elevated temperature data, shown in figure 11, indicated a repeatability of <20 micro-strain. The repeatability of the cryogenic temperature data, shown in figure 12, was <5 micro-strain. As shown in figure 11 and figure 12, there was a difference in output at any given temperature during the temperature excursion. The difference generated was a result of whether the data at a given temperature were recorded during the heat-up or cool-down portion of the apparent strain run. For this paper, this difference in output at a given temperature is stated as hysteresis. It is felt that this hysteresis was primarily caused by the fact that strain data were being recorded as the test beam temperature was changing, and thermal equilibrium throughout the beam thickness was not achieved. The temperature recorded by the PRT on the beam surface, therefore, was not representative of the actual temperature of the strain gage. The exception to this was at the minimum and maximum temperatures where the test beam temperature was allowed to reach thermal equilibrium. The apparent strain characterization testing was performed to determine the general profile of the fiber-optic sensor outputs as a function of temperature change as well as the repeatability of such profiles. Therefore, the ability to achieve thermal equilibrium for each data point was not considered essential. The data represented in figures 11 and 12 were the residual differences between the raw data and a second-order polynomial fit to those data. Figures 11 and 12 demonstrate that the repeatability of fiber-optic gages is based on the scatter in those data. Typical apparent strain signatures for resistance strain gages are linear over a much smaller temperature range. There is a potential benefit from the fiber-optic gage's linear apparent strain. If given apparent strain data for a particular fiber-optic gage with a given material over a given temperature range, the apparent strain for temperatures outside this region could be extrapolated. The apparent strains quoted in this paper are only relative to the particular fiber-optic gage tested and the material on which it was tested.

Load Data and Apparent Strain Conclusions

The results of the room temperature load tests that were conducted on test beams (69C and 78C) with the "improved" fiber-optic strain gages from Luna Innovations, Inc. indicated that the measured strain between the resistance and fiber-optic strain gages, for a given stress, differed by 1.2 to 12.5 percent. Compared to the 25 to 30 percent differences measured during phase 1 testing, it is evident that improvements during the manufacturing process of the fiber-optic strain gages improved the fiber-optic gage's ability to actually measure strain with some degree of accuracy. The strain measurements made with the fiber-optic strain gages installed and tested on the two constant strain test beams, shown in table 2.2, differed from the resistance strain gages by 4 to 9 percent. The data obtained with the three fiber-optic strain gages that were installed adjacent to one another on the constant strain test beam (200-3)

indicated strain measurement variations among the three gages of 2.3 percent (fig. 5). It is felt that these variations in the measured strain values from the fiber-optic gages are caused by the manufacturer's inability to accurately quote the actual gage factor for a given gage.

Table 2.2. Phase 2 Constant Strain Test Beam Load Data

Test beam	Cal. (με)	K990482 (με)	K990483 (με)	K990484 (με)	K990508 (με)	K990509 (με)	K990510 (με)	Resistance gage
200-2	2946	3207	-	3102	-	-	-	2986
200-3	3024	-	3108	-	3147	3143	3227	2964

Although the thermally generated output of the fiber-optic gage was slightly larger at elevated temperatures than at cryogenic temperatures, this output is relatively linear. The typical apparent strain curves generated on resistance strain gages exhibit a nonlinear response. The apparent strain curves on the fiber-optic strain gages that were tested were repeatable to within 5 micro-strain at cryogenic temperatures and to within 20 micro-strain at elevated temperatures. The linear output response of the fiber-optic (F-O) gages to temperature changes allows for apparent strain corrections simply by knowing the slope and the temperature of the gage.

Concluding Remarks

One type of commercially available fiber-optic strain gage from one manufacturer has been evaluated in terms of performance characteristics when compared to conventional foil-type resistance strain gages. Comparative testing included load testing at room temperature and apparent strain testing cryogenically and at elevated temperatures. Note that the data reported in this paper are measurements that compare the strain readings between two types of strain measuring devices. There was no effort at determining the absolute accuracy of either type of strain gage. This evaluation was performed in two phases. During initial testing of the fiber-optic gage, the manufacturer offered an "improved" version of the gage. Both the originally procured gages and the improved gages were subsequently evaluated. Data generated indicated that the second generation (the improved version) fiber-optic gage from the manufacturer did indeed perform substantially better than the originals. The Extrinsic Fabry-Perot Interferometric (EFPI) fiber-optic strain gages proved to be very robust, reliable gages. The fiber was quite flexible and easy to manage throughout the installation and testing processes. Seventeen fiber-optic gages were installed in support of this effort, and none failed or were damaged during the testing. The improvements that the manufacturer implemented as part of their "improved" fabrication process for the fiber-optic gage greatly improved the gage's ability to produce strain readings more closely in agreement with the conventional gages. Although the improvements reduced the differences in the strain measured with each gage type, the fiber-optic gage, on average, measured approximately 6 percent higher strain than the strain measured with the resistance gages. The fiber-optic gages proved to be very repeatable, $\leq \pm 0.2$ percent based on a nominal full-scale output of 3000 micro-strain. Based on what appear to be inaccuracies in the stated gage factor, which affects the overall performance of this particular type of fiber-optic gage, it would be advantageous to determine the gage factor of each gage, that is, calibrate each gage for sensitivity to strain before use. A potential method for determining this gage factor is being investigated.

References

1. Tran, Tuan A.: Stabilized Extrinsic Fiber-Optic Fizeau Sensor for Surface Acoustic Wave Detection. Journal of Lightwave Technology, vol. 10, no. 10, October 1992.

2. Tran, Tuan A., et al.: Absolute Strain Measurements Using the Extrinsic Fabry-Perot Interferometer. Optical Fiber Sensor-Based Smart Materials and Structures Conference, Blacksburg, VA, April 1993.

3. Claus, R., et al.: Extrinsic Fabry-Perot Sensor for Strain and Crack Opening Displacement Measurements From –200 to 900°C. Smart Materials and Structures, vol. 1, p. 237, 1992.

4. Bacon, Fredrick: The Mechanical Strength of Silica Optical Fibers. Silica Optical Fibers Application Note. 3M Fiber Optics Laboratory, June 1995.

5. Moore, Sr., Thomas C.: *Recommend Strain Gage Application Procedures for Various Langley Research Center Balances and Test Articles.* NASA TM-110327, 1997.

6. Shigley, Joseph E.; and Mitchell, Larry D.: Mechanical Engineering Design, Fourth Edition. McGraw-Hill Inc., New York, 1983.

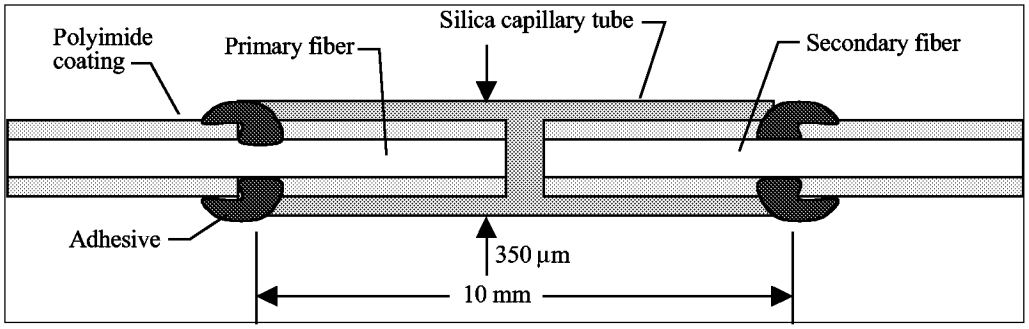

Figure 1. Diagram of EFPI fiber-optic strain gage.

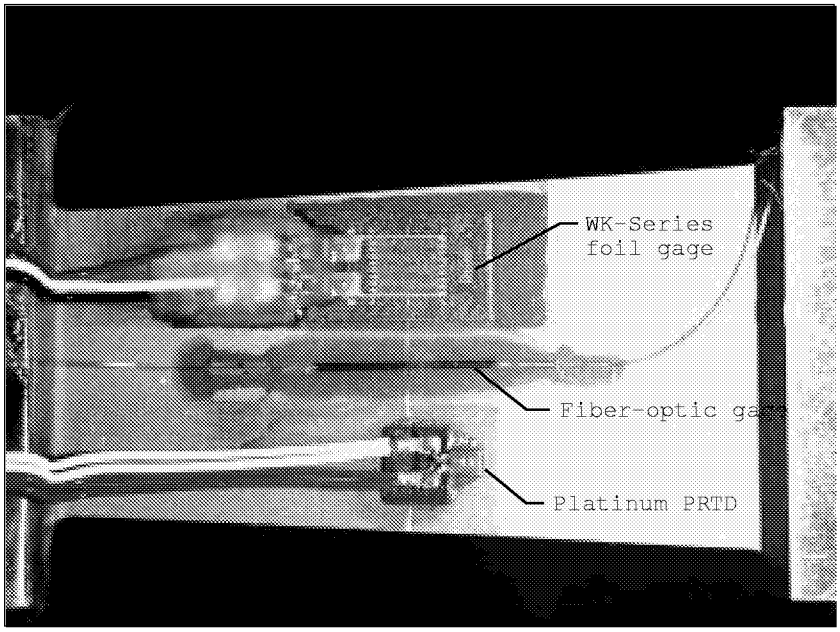

Figure 2. Resistance gage and EFPI fiber-optic gage on test beam. PRTD is a platinum resistive temperature device.

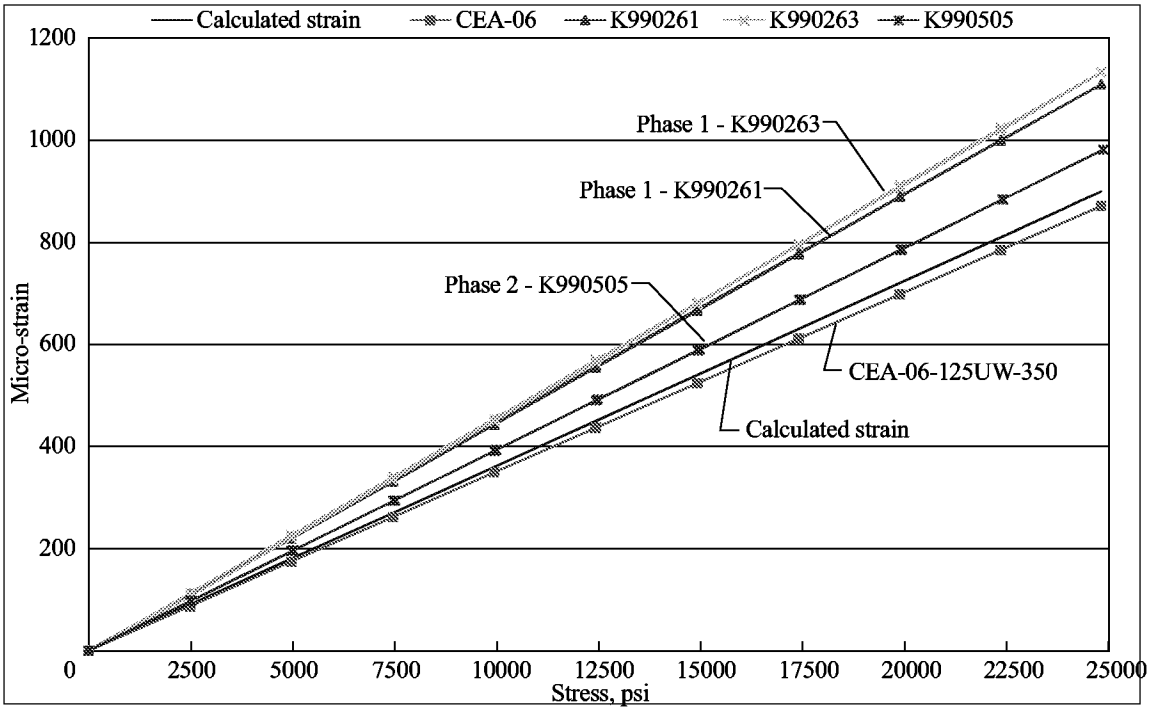

Figure 3. Phases 1 and 2: Comparison of F-O gages and a resistance gage room temperature load data on test beam (69C).

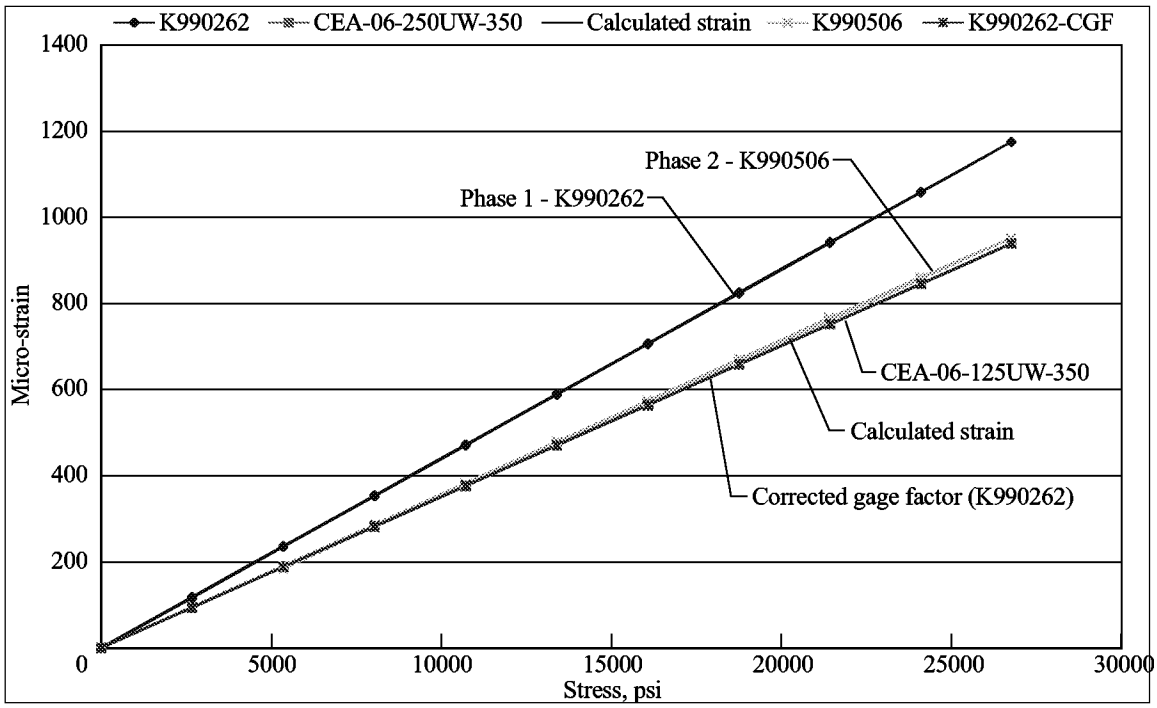

Figure 4. Phases 1 and 2: Comparison of F-O gages and resistance gage room temperature load data on test beam (78C).

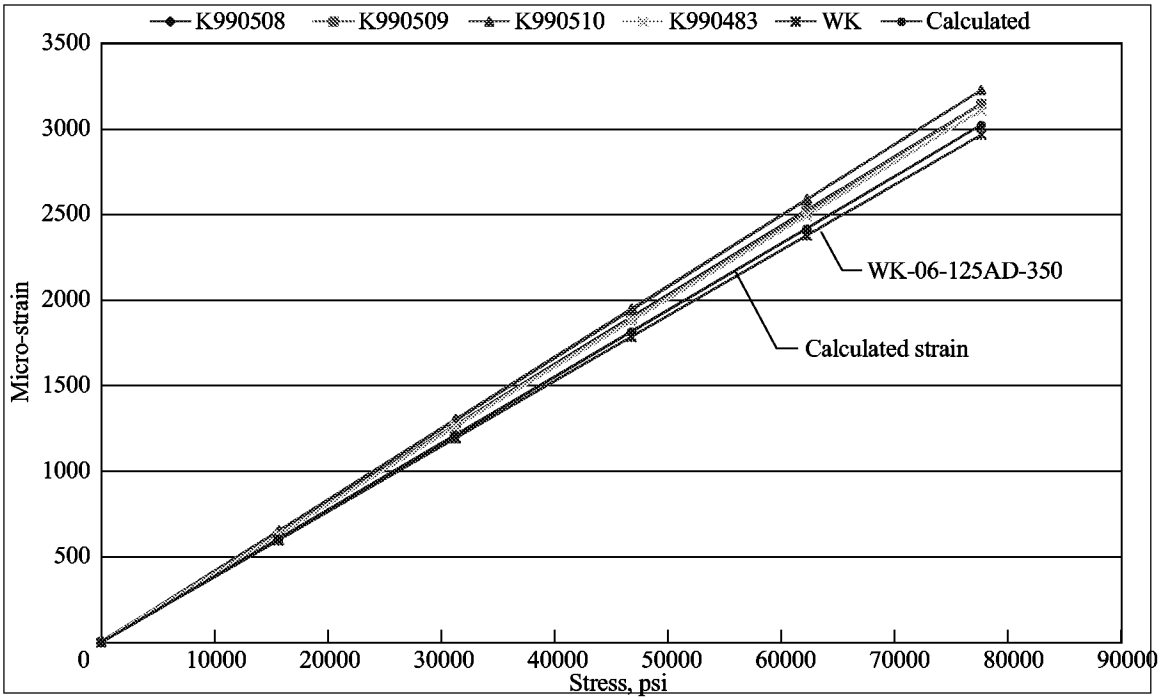

Figure 5. Phase 2: Comparison of F-O gages and resistance gage room temperature load data on test beam (200-3). K99058, K990509, and K990510 were tested in compression; absolute values are shown for comparison with resistive gage WK-06-125AD-350.

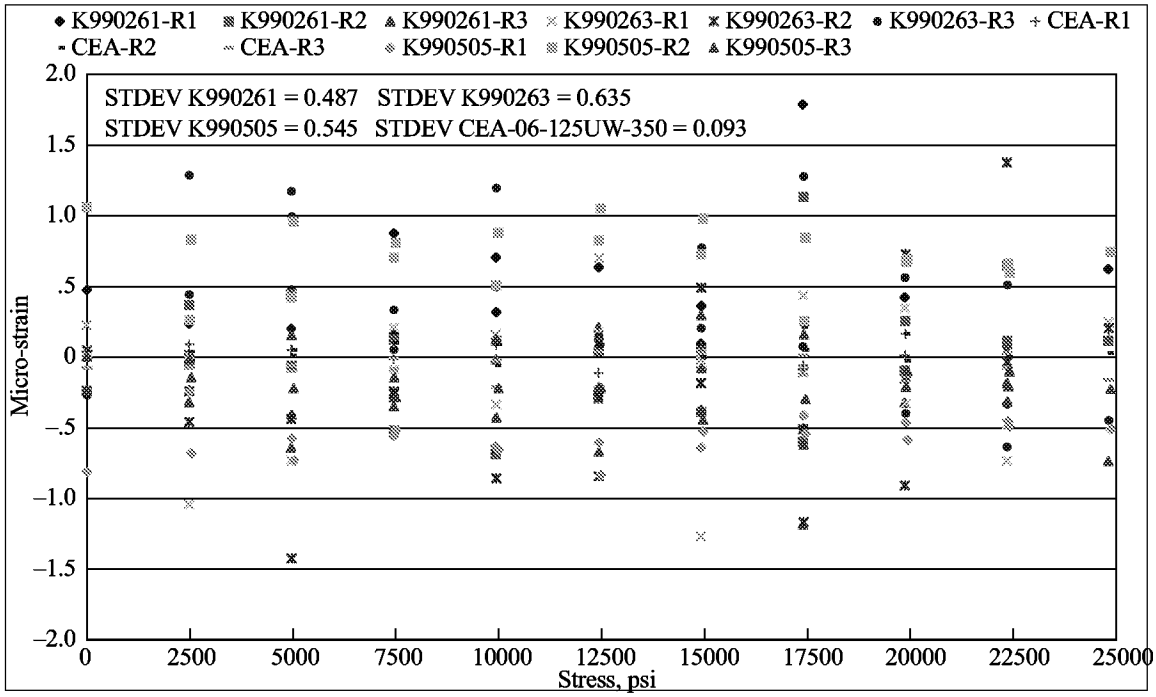

Figure 6. Phases 1 and 2: F-O Gages and resistance gage variation in room temperature load data on test beam (69C).

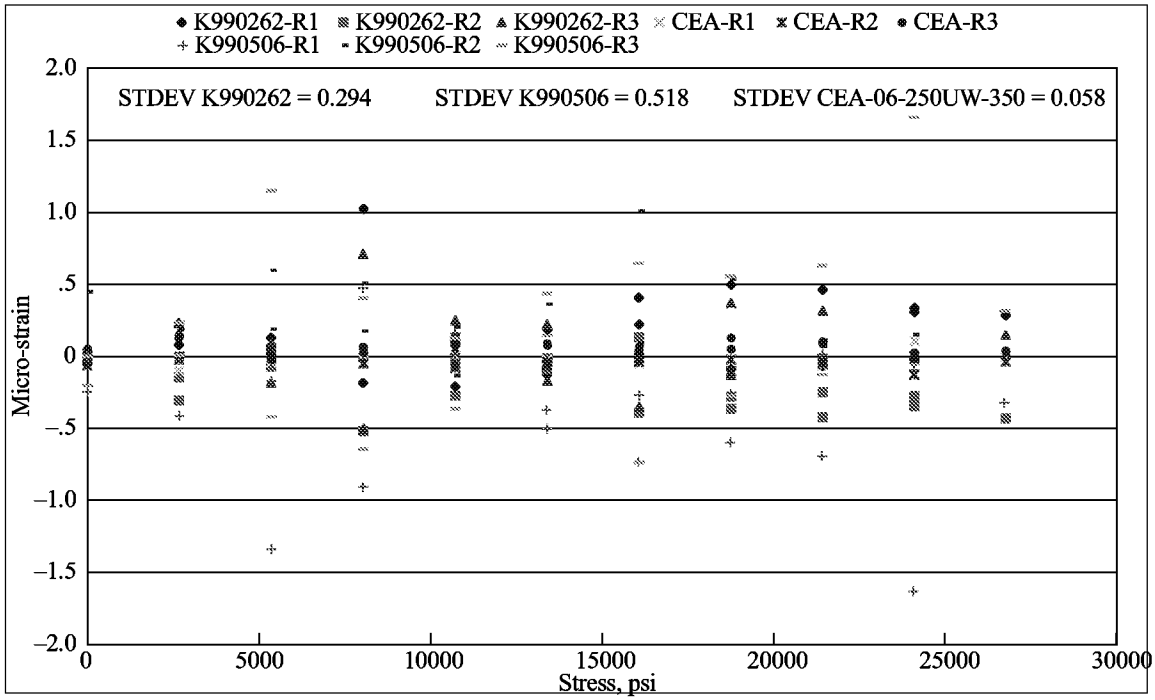

Figure 7. Phases 1 and 2: F-O gages and resistance gage variation in room temperature load data on test beam (78C).

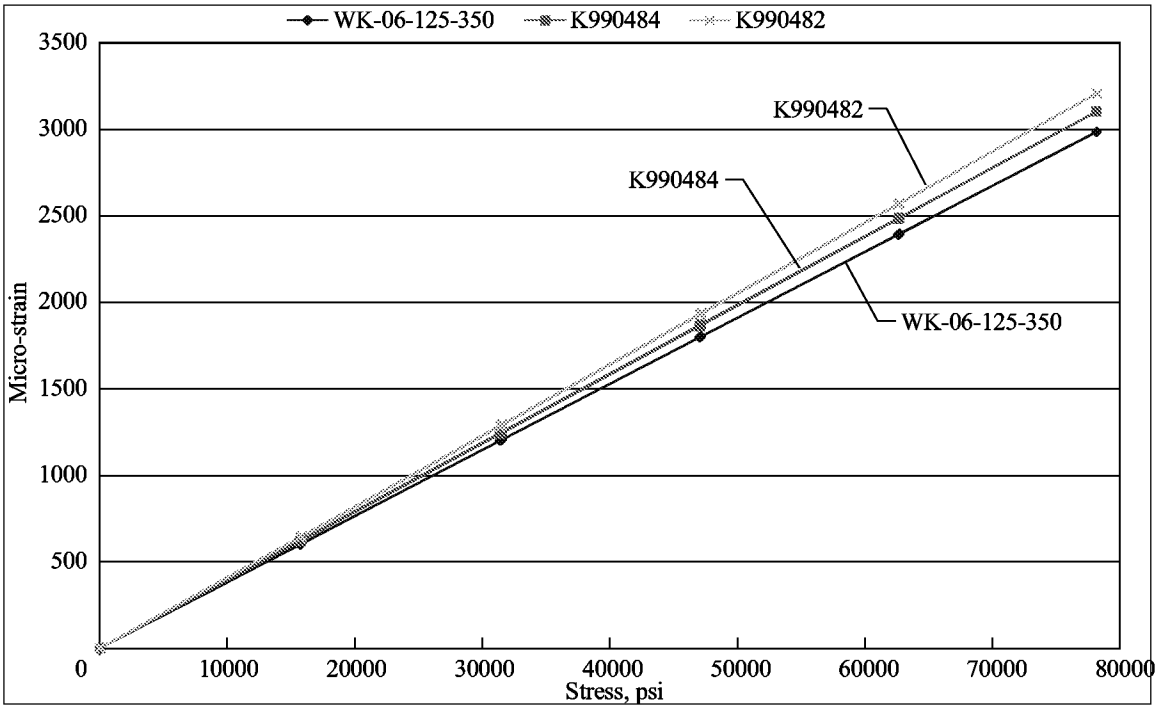

Figure 8. Phase 2: Comparison data of F-O gages and resistance gage room temperature load data on test beam (200-2).

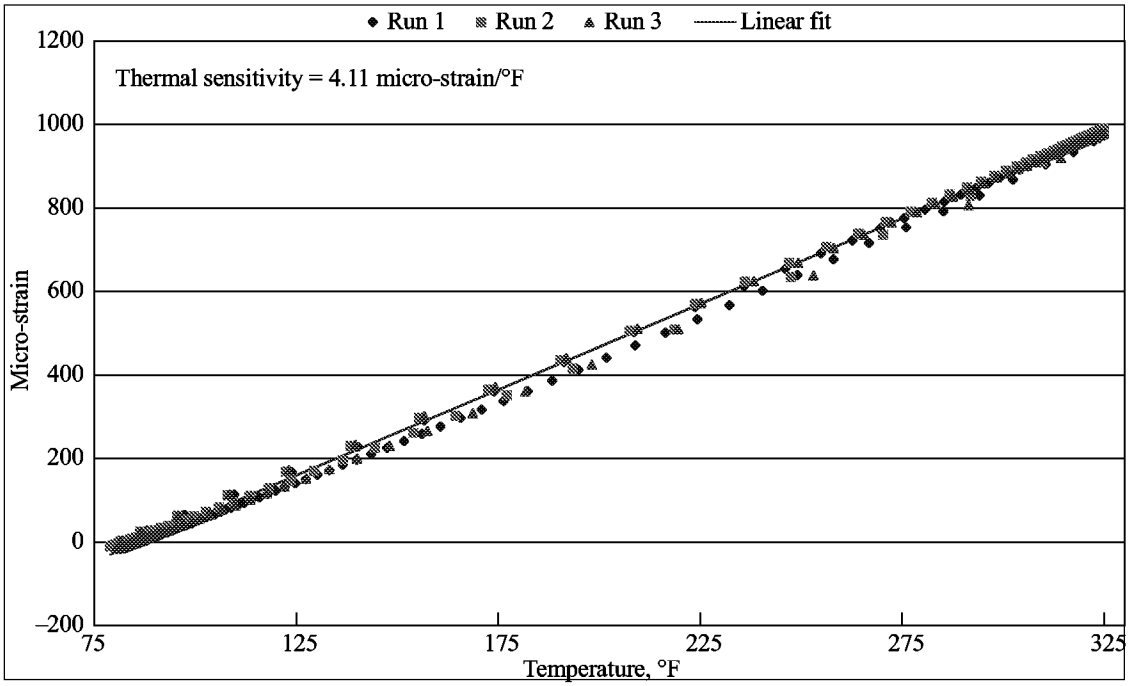

Figure 9. Phase 2: Elevated temperature apparent strain data on F-O gage (K990484) on test beam (200-2).

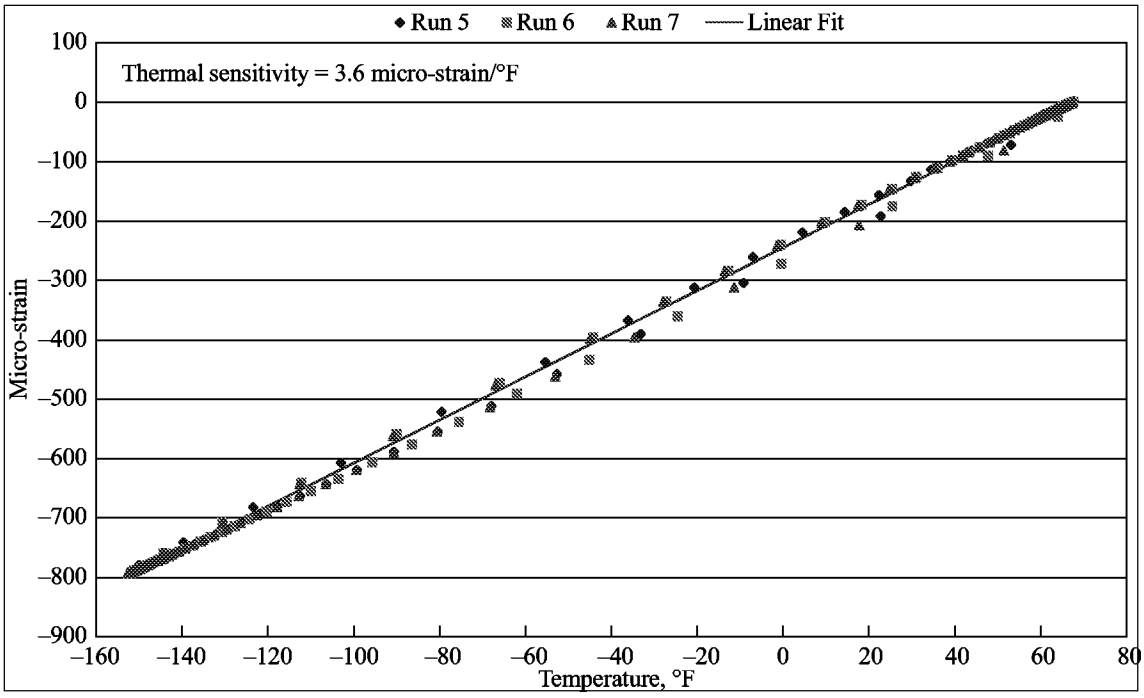

Figure 10. Phase 2: Cryogenic apparent strain data on F-O gage (K990484) on test beam (200-2).

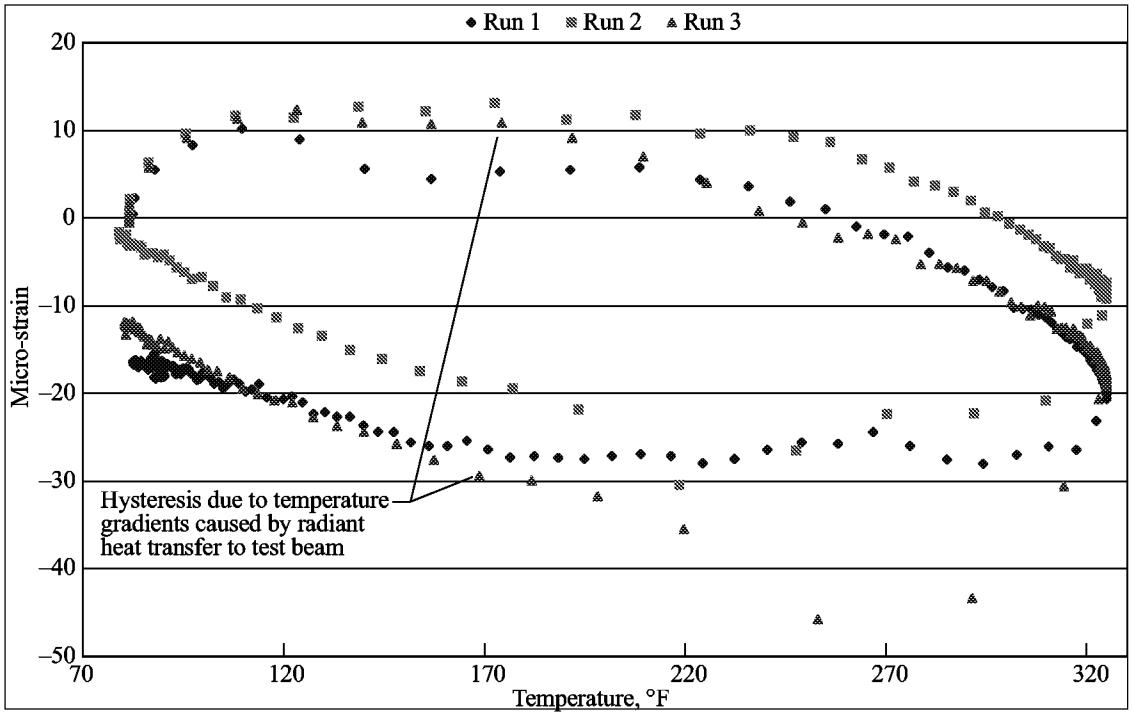

Figure 11. Phase 2: Repeatability of F-O gage (K990484) elevated temperature apparent strain data on test beam (200-2).

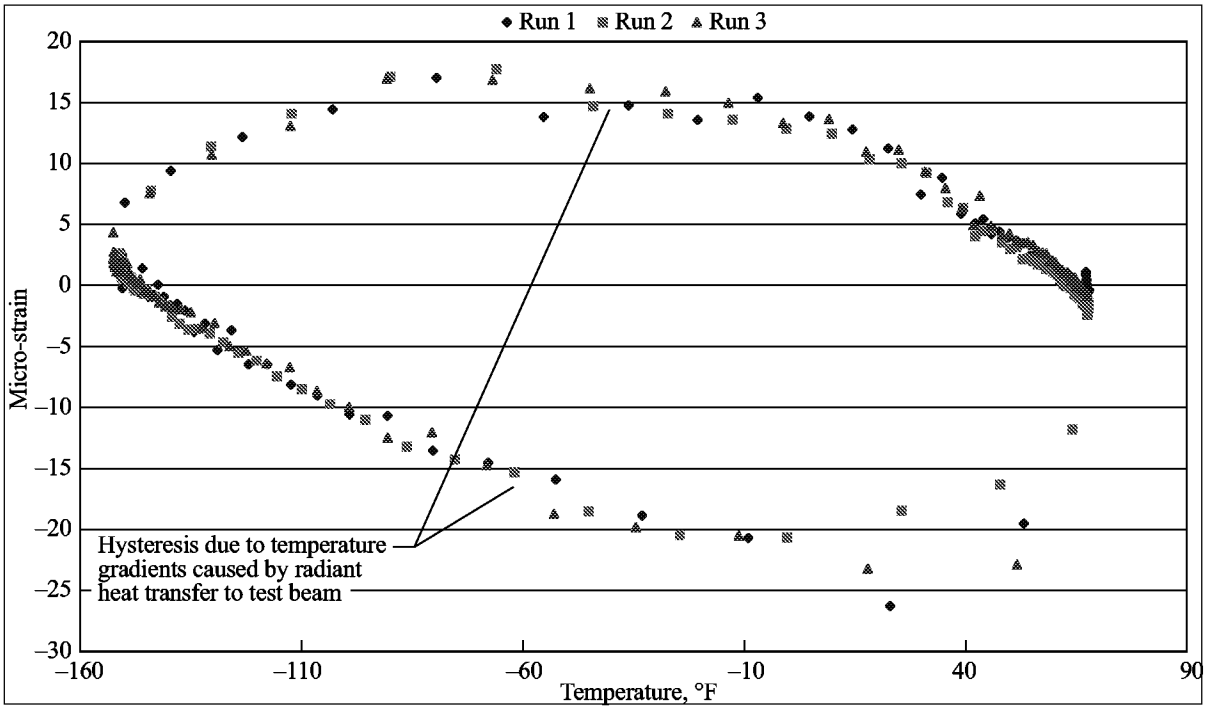

Figure 12. Phase 2: Repeatability of F-O gage (K990484) cryogenic temperature apparent strain data on test beam (200-2).

REPORT DOCUMENTATION PAGE

Form Approved
OMB No. 0704-0188

1. AGENCY USE ONLY (*Leave blank*)	2. REPORT DATE	3. REPORT TYPE AND DATES COVERED
	December 2000	Technical Publication

4. TITLE AND SUBTITLE
Characteristics of Extrinsic Fabry-Perot Interferometric (EFPI) Fiber-Optic Strain Gages

5. FUNDING NUMBERS
WU 706-13-31-05

6. AUTHOR(S)
David A. Hare and Thomas C. Moore, Sr.

7. PERFORMING ORGANIZATION NAME(S) AND ADDRESS(ES)
NASA Langley Research Center
Hampton, VA 23681-2199

8. PERFORMING ORGANIZATION REPORT NUMBER
L-17979

9. SPONSORING/MONITORING AGENCY NAME(S) AND ADDRESS(ES)
National Aeronautics and Space Administration
Washington, DC 20546-0001

10. SPONSORING/MONITORING AGENCY REPORT NUMBER
NASA/TP-2000-210639

11. SUPPLEMENTARY NOTES

12a. DISTRIBUTION/AVAILABILITY STATEMENT
Unclassified-Unlimited
Subject Category 35 Distribution: Standard
Availability: NASA CASI (301) 621-0390

12b. DISTRIBUTION CODE

13. ABSTRACT (*Maximum 200 words*)
For years, resistance based strain sensors have been used for the measurement of strain. The resistance-type strain gage provides a very reliable and accurate measurement of strain, but as with any instrument it has its limitations. Extrinsic Fabry-Perot Interferometric (EFPI) fiber-optic strain sensors are now commercially available from several manufacturers. Fiber-optic strain gages have stated advantages over resistance based strain gages, including immunity to electromagnetic interference (EMI) and leakage to ground. This paper presents a limited performance comparison between the (Fabry-Perot type) fiber-optic strain gage and the traditional resistance strain gage. The evaluation was limited to load testing at room temperature and apparent strain characterization cryogenically and at elevated temperatures. The fiber-optic strain gage evaluation was limited to gages produced by one manufacturer.

14. SUBJECT TERMS	15. NUMBER OF PAGES
Fiber-optic; Gage; Strain; Resistance; Data	22
	16. PRICE CODE: A03

17. SECURITY CLASSIFICATION OF REPORT	18. SECURITY CLASSIFICATION OF THIS PAGE	19. SECURITY CLASSIFICATION OF ABSTRACT	20. LIMITATION OF ABSTRACT
Unclassified	Unclassified	Unclassified	UL